Indian Journal of Natural Products and Resources
Vol. 14(1), March 2023, pp. 112-121
DOI: 10.56042/ijnpr.v14i1.1133

Inhibition of biofilm growth of Gram-positive and Gram-negative bacteria on tuned polyurethane nanofibers

Rumysa Saleem Khan, Taha Umair Wani, Anjum Hamid Rather, Muheeb Rafiq and Faheem A Sheikh*
Nanostructured and Biomimetic Lab, Department of Nanotechnology, University of Kashmir, Srinagar 190006, J&K, India

Received 14 November 2022; revised received 17 February 2023; accepted 23 February 2023

Biofilm formation is a process of bacterial attachment whereby they fasten irreversibly to a biomaterial surface and lead to unwanted phenotypic changes. The chief concern is its formation and to prevent the harmful changes that follow the accumulation of bacteria on implants, so the scientific community has made efforts. In this study, we attempted to fabricate a novel tissue engineering candidate to prevent the biofilm formation desired by ideal biomaterials. We prepared the micro/nanofibers of polyurethane (PU) incorporated with hydrophilic β-cyclodextrin (CD) by electrospinning technique. Further on, these as-spun fibers were in fused with an antibacterial agent. As an antibacterial agent, silver nanoparticles (Ag NPs) were adsorbed on scaffolds. Among the varied methods of its adsorption, adsorption by sonication and hydrothermal process were chosen. Characterization studies performed were scanning electron microscopy (SEM) and water contact angle analysis. The uniform morphology of nanofibers was seen in SEM micrographs which mimics the extracellular matrix. The hydrophilicity test showed the increased hydrophilicity of scaffolds with a decrease in contact angle in CD and Ag NPs incorporated fibre scaffolds. The Ag release assay showed slow release in the case of the fibers where Ag was adsorbed by hydrothermal treatment compared to adsorption by sonication. The antibacterial tests show inhibition of bacteria to different degrees by the fibers. The highest zones were seen in the case of samples with Ag NPs adsorption by sonication. The *in vitro* MTT assay presented that these scaffolds were non-toxic to the cells and could be employed in biological applications.

Keywords: Antibacterial, Biofilm, Electrospinning, Nanofiber, Nanoparticles, Silver

IPC code; Int. cl. (2021.01)- A61P 31/00, A61P 31/04

Introduction

Bacteria bind irreversibly to each other while attaching on a surface and encapsulate themselves in a matrix secreted by them composed of polysaccharide material, ultimately forming a biofilm[1]. The biofilm formation can occur on any biological surface, such as a wound, prosthetic joint, or teeth[2]. In tissue engineering, biofilm formation is a chief concern because it is challenging to remove them from tissue implants, devices and scaffolds[3]. To prevent the harmful changes and infectious diseases that follow the accumulation of bacteria on implants, countless efforts have been made by researchers over the years[4-5]. So, we aimed to fabricate a novel tissue material that can prevent biofilm formation and can be used in tissue engineering applications. Currently, electrospinning is the widely used technique for the fabrication of nanofibers that are used as a potential candidate to replace the traditional dressing material[6]. With the help of electrospinning, these fibers are created from a polymer solution under the influence of an electric field[7]. An electrically charged jet of polymer solution gets deposited on a charged collector in the form of fibers with diameters ranging from nano to micrometers[8]. In this study, we have prepared a micro/nanofiber scaffold of polyurethane (PU) by electrospinning technique. PU is a widely used polymer for fiber fabrication in tissue engineering due to its good mechanical properties, biodegradability, and biocompatibility[9]. The electrospun nanofibers of PU with a large surface area cause the effectual delivery and exchange of fluids and gases into a living surface[10]. However, due to its hydrophobic nature it is mandatory to modify it with certain compounds that improve the wettability of its surface, for which we have blended β-cyclodextrin (CD) in the PU nanofibers. CDs are non-toxic, hydrophilic and cyclic oligosaccharides with a unique cone-shaped molecular structure, forming inclusion complexes with other compounds[11]. This way the drugs, antibacterial agents, and other growth factors are encapsulated within its cage-like structure, allowing their controlled release[12]. The particle and drug loading of fibers for controlled release and better dissolution

*Correspondent author
Email: faheemnt@uok.edu.in

profiles has been studied extensively by different researchers[13-14]. To impart the antibacterial property to the fibers, we intended to incorporate the fibers with silver (Ag) nanoparticles (NPs). There is extensive literature supporting the antimicrobial activity of Ag NPs[8,15–17], so as an antibacterial agent, Ag NPs was adsorbed on scaffolds. There are varied methods of its adsorption on fibers such as, ultraviolet irradiation, embedding Ag NPs into polymer nanofiber by electrospinning, simultaneous reduction of $AgNO_3$ and adsorption of Ag NPs on fiber surface[18–21]. However, these methods do not disperse the NPs well and show the presence of only a few NPs at a particular point on the fibers. In addition to these methods, there are other methods of Ag NPs adsorption such as, adsorption by sonication and hydrothermal processes. These methods are efficient in proper dispersal of Ag NPs on the fibers. The advantage of sonication is the achievement of a very homogeneous coating with a narrow particle size distribution[22-23]. Similarly, the hydrothermal approach of Ag NPs adsorption has been linked to the proper binding and dispersion of NPs with fiber surfaces upon high temperature and pressure[24–27]. So, in this study, these two approaches to analyze the efficiency of the fabricated scaffolds in biofilm stoppage have been used. The present study presents a novel way of inhibition of biofilm formation using modified PU micro/nanofibers whose properties have been tuned by incorporating different biocompatible substances.

Materials and Methods

Materials

Polyurethane (PU) (M_w 110,000, EG-80A, Tecoflex™) was acquired from Lubrizol Corporation (USA). Tetrahydrofuran (THF) and N.N-dimethyl formamide (DMF) were purchased from Sisco Research Laboratories (India). Silver nitrate ($AgNO_3$) and fetal bovine serum (FBS) were purchased from Sigma Aldrich (USA). Sodium borohydride ($NaBH_4$) was purchased from SD fine chemicals Ltd. (India). β-cyclodextrin was purchased from CDH (India). Luria Bertani (LB) broth and agar media were purchased from G-Biosciences (USA). 3-(4,5-dimethylthiazol-2-yl)-2,5-diphenyl tetrazolium bromide (MTT) reagent, dimethyl sulfoxide (DMSO), trypsin-EDTA and antibiotics 5,000U penicillin/ streptomycin were purchased from HighMedia Laboratories (India). Dulbecco`s modified eagle`s medium (DMEM) was obtained from Lonza (Switzerland). The model bacteria used in the study were *Staphylococcus aureus* (ATCC 2913) and *Escherichia coli* (DH5α) and were kindly provided by IIIM, Srinagar. The mouse fibroblasts 3T3 L1 were obtained from Cell Lines Service (Germany).

Preparation of CD-incorporated PU micro/nanofibers

The solution for fabrication of fibers was prepared by dissolving 12 g of PU in THF under constant stirring using hot plate stirrer at 80 RPM. Following this, 5 wt% CD (with respect to the weight of the polymer) was dissolved in DMF. This solution was added to the polymer solution (initially prepared using THF) to give a final 9:1 THF and DMF ratio. After the preparation of the polymeric solution, the electrospinning was carried out in a 10 mL syringe. The distance between the tip of syringe needle and the collector was set at 15 cm, and the voltage and temperature were set at 13 kV and 30ºC, respectively. After refilling the syringe 3-4 times during the process, a thick mat of micro/nanofibers was obtained on the aluminum foil that was wrapped on the collector before electrospinning. The mat was dried overnight in a hot-air drier for 12 h.

Adsorption of silver nanoparticleson the scaffolds

For the preparation of Ag NPs, the precursor used was $AgNO_3$. Exactly 10 wt% of $AgNO_3$ was weighed with respect to the pre-weighed 5 cm × 5 cm as-spun micro/nanofiber mats. To this, 20 mL of distilled water was added and two solutions of $AgNO_3$ were prepared in separate falcon tubes. Then, the 0.5M $NaBH_4$ solution was prepared to reduce the Ag^+ ions in $AgNO_3$ which was added in equal volumes to the two solutions of $AgNO_3$. The reduction was carried out for 12 h under constant agitation in a shaking incubator. After the transition of colour of $AgNO_3$ solutions from colourless to black, the reduction was confirmed. Two 5cm×5cm micro/nanofiber mats were immersed in the two $AgNO_3$ solutions and were subjected to two different methods of adsorption. For sonication, the tube containing the mat immersed in reduced $AgNO_3$ solution was exposed to sonic vibrations for 1 h at a temperature of 30ºC in an ultrasonic homogenizer. For this, the sonicator was first filled to half of its capacity with distilled water and the temperature was maintained at 30ºC. Following this, the tube was set in proper alignment so that the part containing the fiber mat that was immersed in $AgNO_3$ solution was in contact with the water for the penetration of ultrasonic vibrations. Finally, the fiber mats were transferred to a glass petri plate and left to dry in a hot-air drier overnight.

For the adsorption of Ag NPs by hydrothermal treatment, the tube contents, after pre-wetting, were transferred to the Teflon cup of a hydrothermal reactor. Following this, the reactor was closed and tightly sealed and placed in an oil bath for 1 h at 80ºC. After the completion of reaction, the reactor was taken out of the oil bath and placed in an ice bath to bring the temperature down. Finally, the reactor was opened, and the fiber mat was transferred to a petri plate and left to dry for 12 h. At the end of the adsorption processes, three types of scaffolds were obtained, i.e., pristine CD incorporated PU scaffold without any doped Ag NPs (PU/CD), the PU/CD scaffold with adsorbed Ag NPs by sonication (AgSON) and the PU/CD scaffold with adsorbed Ag NPs by hydrothermal treatment (AgHYD).

Characterization

Field emission scanning electron microscopy (FE-SEM) coupled with energy-dispersive X-Ray spectroscopy (EDS) was used to analyze the morphology of the fabricated fibers. For the sample preparation, the fiber mats were first completely dried and were then sputter coated with gold ions for 5 min. After the samples were loaded in the FE-SEM unit, the electron beam was passed through the electron gun and the micrographs were taken at different magnifications. The diameter distribution of nanofibers and the size of NPs were calculated from these images. Also, the EDS analysis gave the elemental distribution of fiber mats and confirmed Ag NPs. To check the effect of CD on the hydrophobicity of PU, the contact angle analysis was carried out. For this, a drop of water was placed on each fiber scaffold, and the droplet images were captured in all cases simultaneously using the contact angle meter. These images were then analyzed in ImageJ software, having the contact angle extension to measure the angles in triplicates. The measurements were then plotted in the form of a line graph.

Silver release assay

Both the AgSON and AgHYD scaffolds were cut into 2 cm × 2 cm strips and immersed in 20 mL distilled water in falcon tubes. The tubes were incubated for different time points at 37°C under constant agitation in a shaking incubator for 5 days. On the completion of incubation times, the required amount of solution from the tubes was taken and analyzed in a UV-Vis spectrophotometer and the volume of tubes was made the same again by adding an equal amount of distilled water. For the absorbance measurements, first, the spectrum for $AgNO_3$ solution reduced with $NaBH_4$ was obtained in the range of 200-800 nm using a UV-Vis spectrophotometer using distilled water as blank. Then the wavelength of the highest absorbance was obtained, i.e., 420 nm. The absorbance for sample solutions was taken at this wavelength on completion of incubation periods, i.e., 1, 2, 3, 4 and 5 days and the measurements were plotted.

Antibacterial assay

The scaffolds were tested for antibacterial activity against two model microbes, *Staphylococcus aureus* and *Escherichia coli*, by disk diffusion assay and growth curve analysis. For the disk diffusion assay, the bacterial strains were cultured in LB broth under constant shaking and an optimum temperature of 37ºC for bacterial growth till the absorbance of the culture solution reached 0.4-0.5. For the preparation of solid growth media, the LB agar solution was prepared and autoclaved. The agar plates were prepared by pouring the sterile hot agar solution on bacterial culture plates and were left to solidify by cooling. For the sample preparation, all the fiber scaffolds were punched into circular disks under sterile conditions using a biopsy puncher with outer and inner diameters of 8 and 7 mm respectively. These disks were incubated in 70% ethanol for 1 h followed by washing with saline solution to remove ethanol from scaffolds and were left to dry in a hot-air drier. The agar plates' surface was inoculated with a plastic spreader with 10 µL of above prepared bacterial cell suspension. The sterilized disks of all samples, i.e., PU/CD (negative control), ampicillin immersed filter paper disks (positive control), AgSON, AgHYD, and Ag NPs solution immersed filter paper disks (for comparison), were carefully placed on the agar plates using the sterilized forceps. Finally, the plates were incubated at 37°C for 12 h and the diameters of the circular hollow zones on the bacterial lawns were measured using ImageJ software in triplicates.

For growth curve analysis, the liquid bacterial cultures of *S. aureus* and *E. coli* were grown until the OD of 0.4 was reached. Then a volume of 100 µL of this culture was added to 10 mL of fresh broth in different tubes. Following this, small strips (1 cm × 1 cm) of all scaffolds were immersed in these tubes for 12 h and were incubated at 37°C under constant shaking. The OD values were measured after every 2 h of incubation for 12 h using a UV-Visible spectrophotometer at a wavelength of 600 nm. As a positive control, the tube containing broth inoculated

with 100 µL of bacterial culture was used and as negative control, the broth without any inoculum was used. This also gave an idea of contamination in the culture conditions. In addition to this for comparison purposes, 1cm × 1cm strips of filter paper were taken and immersed in ampicillin solution for 10 min followed by drying and immersing in another tube of bacterial culture inoculated broth. After the procurement of OD measurements line graphs were plotted and the bacterial growth curves were obtained for all samples and the growth patterns were analyzed.

Cell toxicity analysis

To check the viability of cells on the fiber scaffolds, mouse 3T3 L1 cells were cultured for different incubation periods on the scaffolds. First, the fiber scaffolds were punched to form circular disks using a biopsy puncher (outer diameter = 6 mm and inner diameter = 5 mm) under aseptic conditions. These disks were then placed in the wells of 96-well plates. These were ethanol sterilized for 1 h followed by washing with PBS. Following this, the wells were filled with 100 µL of complete media containing 10% FBS, 1% Penicillin-Streptomycin antibiotic and DMEM. Then, cells were seeded on the fibers at a density of about 2×10^5 cells/well for 1, 2, and 3 days of incubation at 37ºC and under a constant supply of 5% CO_2. The exhausted media was replenished every day of the culture. On the completion of incubation time, the media was removed from all the wells, followed by the addition of 100 µL DMEM and 50 µL MTT reagent (0.5 mg/mL). The plates were incubated for 2hand the yellow-coloured MTT reagent was reduced to purple-coloured formazan crystals by mitochondrial oxidases. After 2 h, these crystals were solubilized with 50 µL of DMSO and incubated at 37ºC for 30 min. The absorbance of the final solution was read at 560 nm using a microplate reader and converted to cell viability % using the following formula.

$$Cell\ viability\ (\%) = \frac{Sample\ absorbance - Blank\ absorbance}{Control\ absorbance - Blank\ absorbance} \times 100$$

Results and Discussion

Characterization

The morphology of the fabricated as-spun microfibers was analyzed using SEM and the micrographs obtained at different magnifications are shown in Fig. 1. It can be seen from these results that the fibers were of uniform morphology and no beads were seen concluding the successful electrospinning of fibers. As desired, no NPs were seen in the case of PU/CD fibers (Fig. 1a-d). However, these NPs were clearly seen in the AgSON (Fig. 1b-e) and AgHYD fibers (Fig. 1c-f). The Ag NPs adsorbed by sonication showed an equal distribution on the fibers and the average size of NPs was found to be 199.9±68.7 nm.

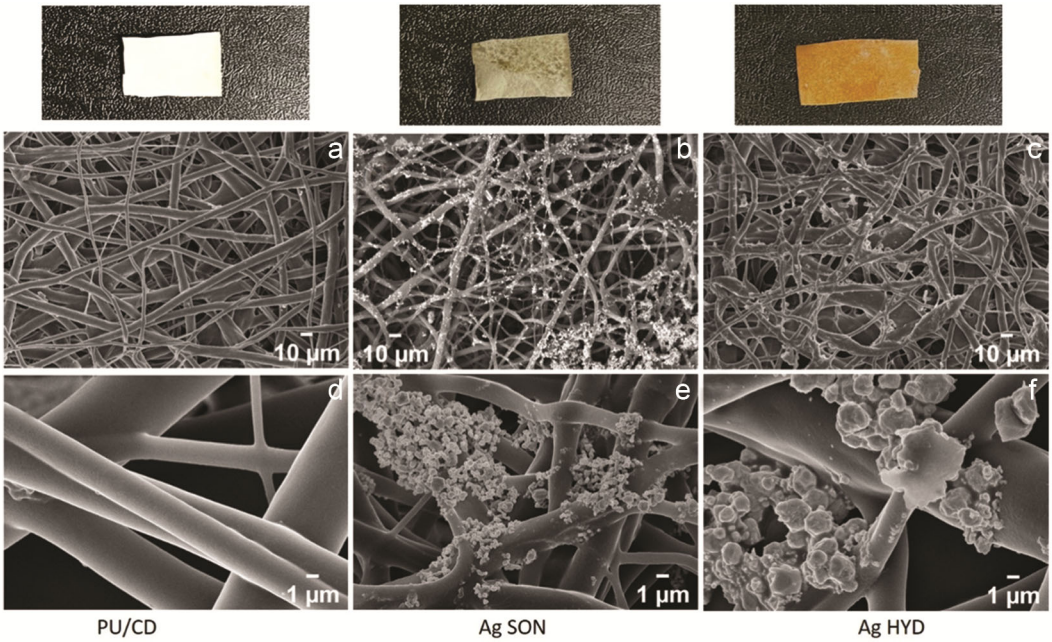

Fig. 1 — The SEM micrographs at two different magnifications of the electrospun, a-d) Pristine PU/CD scaffolds; b-e) PU/CD fibers with adsorbed Ag NPs by sonication; and c-f) PU/CD fibers with adsorbed Ag NPs by hydrothermal treatment.

In contrast, Ag NPs adsorbed by hydrothermal treatment showed uneven distribution with clumping at most places and the average size of NPs was found to be 47.7±43.9 µm, much larger than the former ones. The reason for this could be the clumping of Ag NPs together under the influence of high temperatures leading to the larger size of NPs or the growth of NPs after nucleation sites are set in the reactor. The diameter distribution of fibers is given in Fig. 2. The average diameters of PU/CD, AgSON, and AgHYD fibers were 3.9±1.8, 4.0±1.7, and 8.0±2.2 µm respectively. It can be concluded that the hydrothermal treatment has caused a significant increase in the average diameter of fibers. The EDS analysis also confirmed the successful incorporation of Ag NPs in the fibers as shown in Fig. 3. The Ag peak can be seen in both AgSON and AgHYD scaffolds and is absent in pristine PU/CD scaffolds. The element overlay of the scaffolds also shows the presence of Ag NPs in AgSON with even distribution and AgHYD scaffolds with an uneven distribution and total absence in pristine PU/CD fibers. The results declare that the ultrasonic vibrations were more efficient in evenly dispersing Ag NPs on the fibers than the high temperature in a hydrothermal reactor. The hydrophilicity analysis of the scaffolds was carried out to determine whether the surface of the modified nanofibers is hydrophilic on the incorporation of CD. This test also interprets the interference of scaffolds with cell attachment and proliferation. The contact angle measurements are given in Fig. 4. All the samples had a contact angle of less than 90º, which shows the hydrophilicity imparted by CD in all scaffolds. Furthermore, the difference between the contact angles of PU/CD and AgSON scaffolds was 82.7±0.05 and 82.05±0.05º, respectively. The lowest

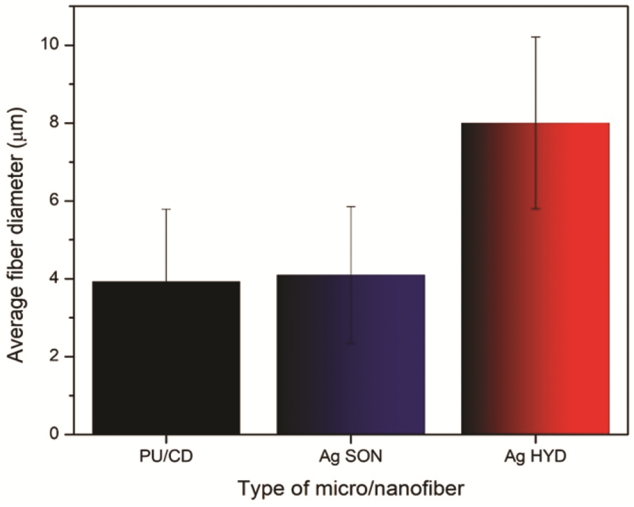

Fig. 2 — The diameter distribution of electrospun PU/CD micro/nanofibers and its composites with adsorbed Ag NPs by sonication (Ag SON) and hydrothermal treatment (Ag HYD).

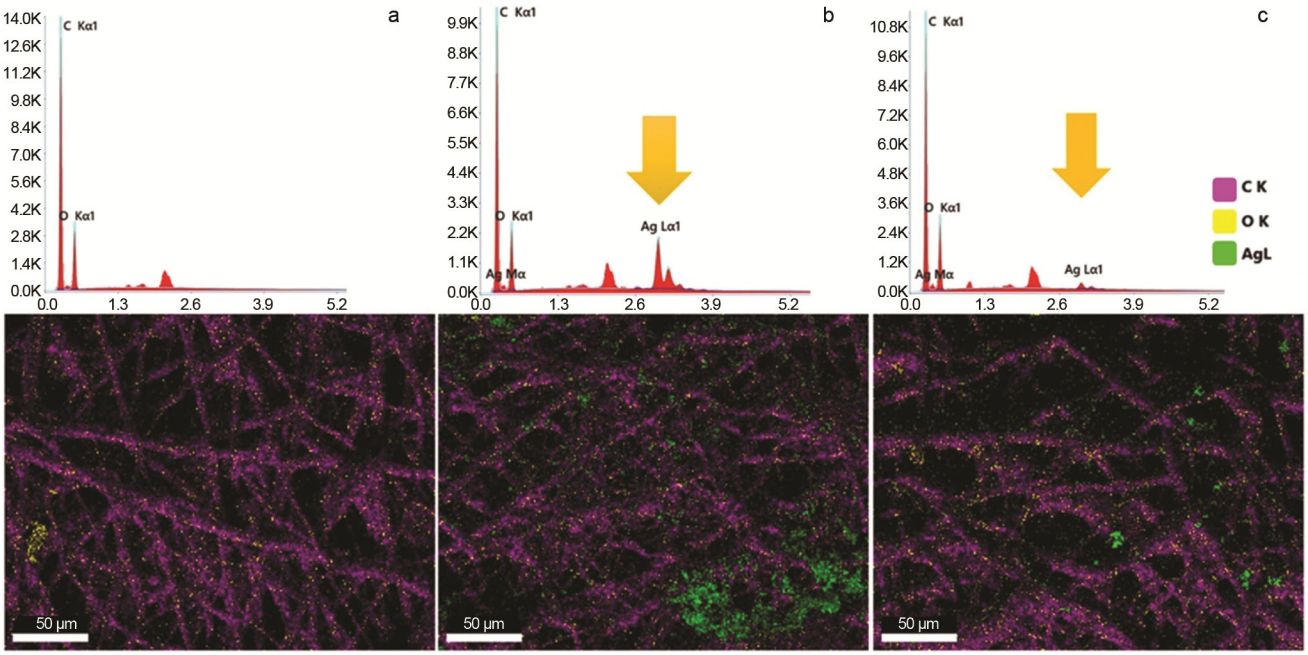

Fig. 3 — The EDS analysis and corresponding element overlay of, a) electrospun PU/CD fibers and its composites with adsorbed Ag NPs by; b) sonication (Ag SON); and c) hydrothermal treatment (Ag HYD).

contact angle was seen in the case of AgHYD scaffolds measuring 68.5±0.2º, which can be attributed to the fact that high temperature changed the morphology of fibers significantly in such a way that the fibers lost the crystallinity and became more hydrophilic.

Silver release assay

The results of release behaviour of Ag NPs from the fibers in AgSON and AgHYD scaffolds from UV spectrophotometry are shown in Fig. 5. The graph indicates that on the first day, there was a full release of Ag NPs from the AgSON samples compared to the AgHYD scaffold. Furthermore, there was a gradual decrease in the release of Ag NPs upon additional incubation, and the release was almost zero on the fifth day in both cases depicting the complete release of Ag NPs from the fibers in 5 days. The high release in the case of AgSON can be attributed to the fact that the NPs were present in high concentration in these fibers due to the excellent adsorption compared to the electrospun AgHYD.

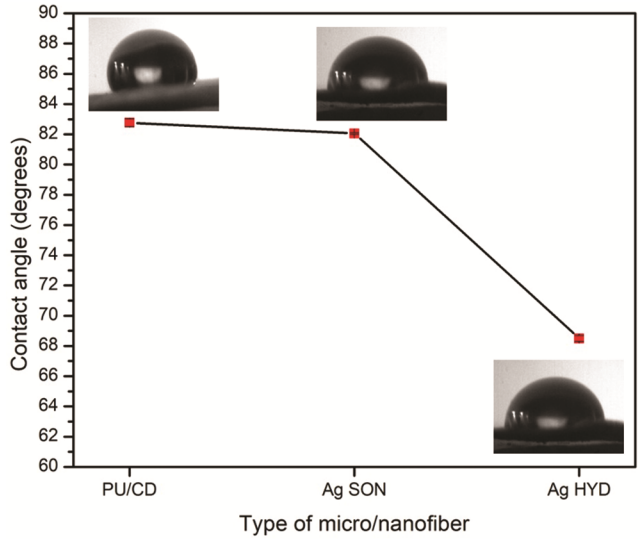

Fig. 4 — The contact angle analysis of the electrospun PU/CD micro/nanofibers and its composites with adsorbed Ag NPs by sonication (Ag SON) and hydrothermal treatment (Ag HYD).

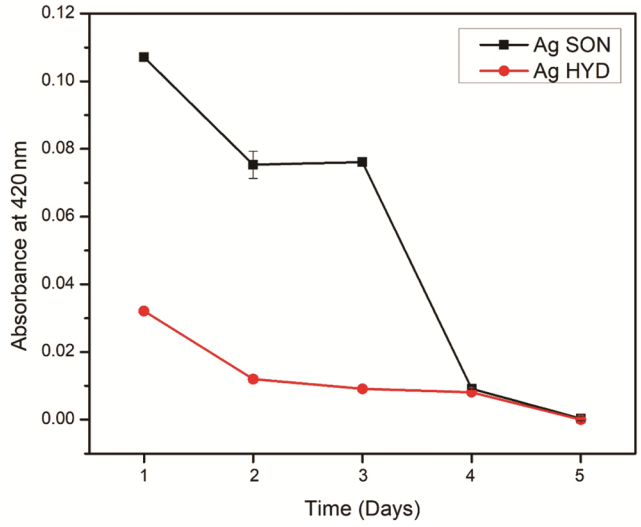

Fig. 5 — The Ag NPs release from the electrospun PU/CD micro/nanofibers with adsorbed Ag NPs by sonication (Ag SON) and hydrothermal treatment (Ag HYD).

Antibacterial assay

To test the antibacterial property of the scaffolds, the disk diffusion assay was carried out. The results in Fig. 6a-b show that the negative control, PU/CD scaffolds did not have any antibacterial activity against any bacterial strain whereas the Ag NPs adsorbed scaffolds had significant antibacterial activity. Also, significant antibacterial activities were seen with the positive control, ampicillin and Ag NPs. Fig. 6c shows the average diameter distribution of the zones of inhibition in the case of all scaffolds against *E. coli* and *S. aureus.* In the case of *E. coli*, the zone of inhibition shown by AgSON was 22±1 mm and by AgHYD was 19.33±0.5 mm concluding AgSON to be a more potent antibacterial scaffold against it. Also, the zone of inhibition shown by positive control, ampicillin in this case was 26.33±0.5 mm and zone showed by Ag NPs was very close to ampicillin equal to 25±1 mm. Similarly, in the case of *S. aureus*, the zone of inhibition shown by AgSON was 24.33±0.5 mm and by AgHYD was 21±1 mm. These results indicate that Gram-positive bacteria are more susceptible to the antibacterial agents than Gram-negative bacteria. Also, the results depict AgSON as the better antibacterial scaffold than AgHYD against *S. aureus* also. This can be attributed to the fact that the size of Ag NPs in the case of AgSON scaffolds is much reduced than AgHYD scaffolds, which penetrate inside the bacterial cells. The zones shown by both ampicillin and Ag NPs in this case were exactly equal (26.33±0.5 mm). This concludes that the Ag NPs were somehow hindered from entering the Gram-negative bacteria and hence showed the less antibacterial effect against them as compared to Gram-positive bacteria. However, the difference between the antibacterial efficiency of ampicillin and Ag NPs is not significant and it can be concluded that Ag NPs are as efficient antibacterial agents against bacteria as the commercial antibiotic ampicillin. Also, from the results, it can be concluded that among the two mats, AgSON is a better choice of fiber scaffold for its use against biofilm formation.

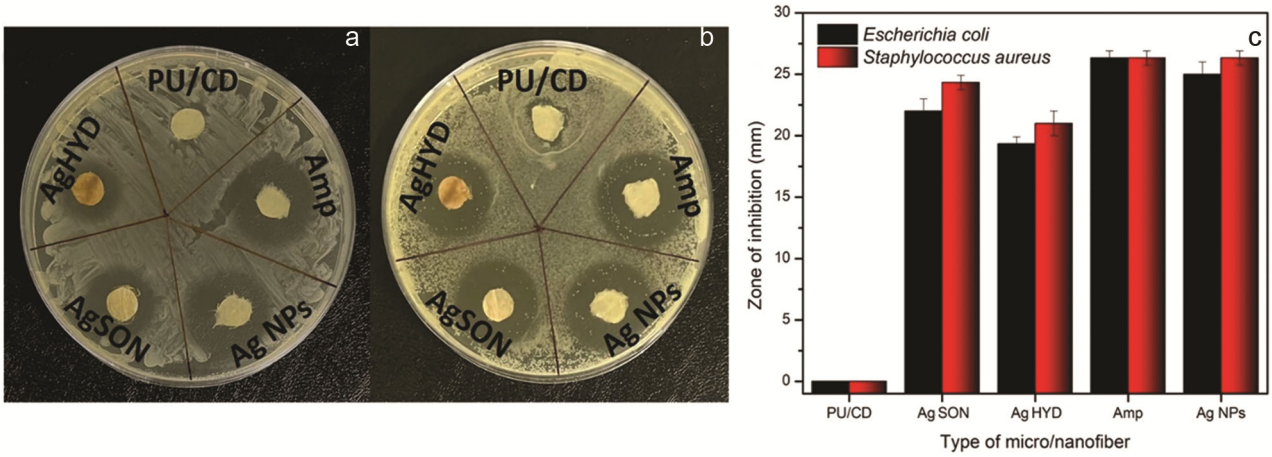

Fig. 6 — The disc diffusion assay against, a) *Escherichia coli*; b) *Staphylococcus aureus* of the electrospun PU/CD micro/nanofibers and its composites with adsorbed Ag NPs by sonication (Ag SON) and hydrothermal treatment (Ag HYD) along with the positive control ampicillin and Ag NPs for comparison; and c) The diameter distribution of the zones of inhibition.

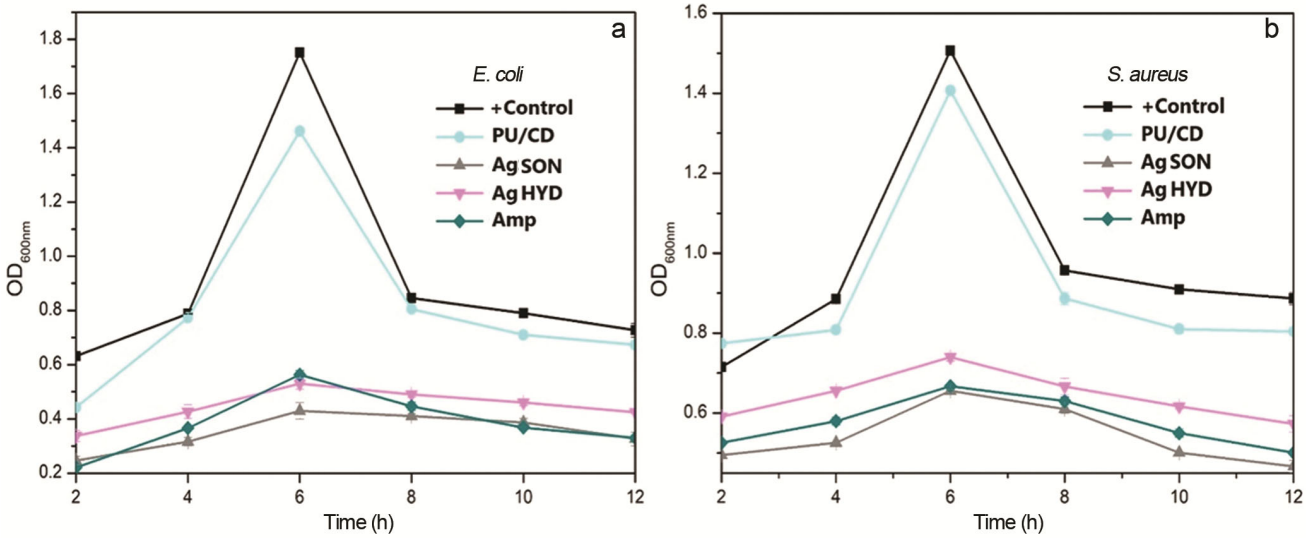

Fig. 7 — Bacterial growth curves obtained after incubation of samples in bacterial cultures of a) *Escherichia coli*; and *b*) *Staphylococcus aureus.*

Furthermore, the OD measurements of the scaffolds immersed in bacterial cultures of *E. coli* and *S. aureus* were taken after every 2 h for an incubation time of 12 h at 600 nm wavelength. The results of the same were plotted in the form of a growth curve and are given in Fig. 7. For *E. coli* (Fig. 7a), the growth curves for positive control and pristine PU/CD scaffolds firstly showed a continuous increase for 6 h and then showed a sharp decrease after further incubation. On the other hand, the Ag NPs adsorbed scaffolds and the ampicillin control also followed the same trend of growth 6 h but the absorbance was significantly lower than the PU/CD scaffold and positive control. Further, incubation of these composites followed a decrease in OD until the end of culture time, i.e., 12 h. In case of *S. aureus* (Fig. 7b), the same pattern of growth curve was seen for all the scaffolds. The OD first increased constantly until 6 h and then gradually decreased until the end of time of incubation in all cases. The OD in case of Ag NPs adsorbed scaffolds and ampicillin control was visibly lower than the PU/CD scaffold and positive control in this case also. The results confirm the successful inhibition of bacteria with the modified PU scaffolds and AgSON curves showed more antibacterial inhibition than AgHYD in both strains (Fig. 7). These results validate our results obtained from disk diffusion assay.

Cytotoxicity assay

To check whether the scaffolds are non-toxic to the cells, the cell viability assay was carried out. Cell viability was calculated from the MTT assay upon

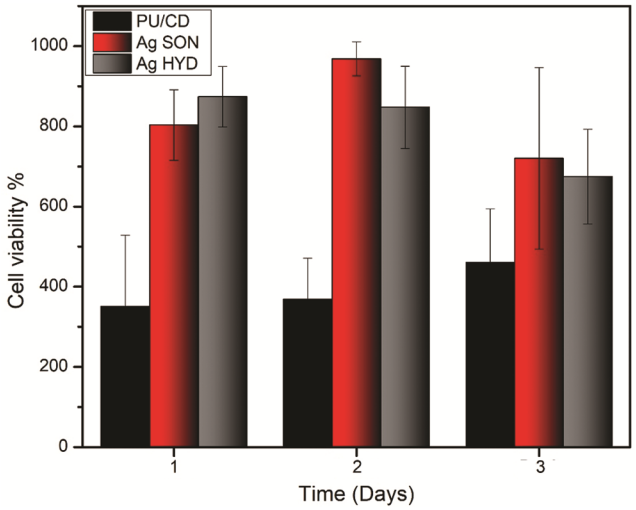

Fig. 8 — The cell viability analysis against 3T3 L1 cells of the electrospun PU/CD micro/nanofibers and its composites with adsorbed Ag NPs by sonication (Ag SON) and hydrothermal treatment (Ag HYD).

3 days of cell culture. The results shown in Fig. 8 indicate the viability % of cells on all the scaffolds. On day 1 of the cell culture, the viability % of PU/CD fiber was 350.61±177.7%, AgSON fiber was 803.23±87.85%, and AgHYD fiber was 873.7±75.4%. On day 2 of the culture, the viability was further increased in all the cases with the viability % of 368.93±102.6, 968.13±42.35 and 847.25±102.77% in the case of PU/CD, AgSON, and AgHYD fibers, respectively. On the last day of culture, i.e., day 3, the cell viability kept on increasing in the case of PU/CD fibers with 460.67±133.5% viability. However, the viability got decreased in the cases of AgSON and AgHYD, with viabilities as 719.98±226.4 and 674.64±118.26% respectively. These results show that the viability of all scaffolds is above 200% on all days of culture, which means that all scaffolds are non-toxic to cells. Furthermore, on day 3, the decline in cell viability on AgSON and AgHYD scaffolds as compared to other days of culture may be due to the accumulation of Ag NPs in the culture media, which might be toxic due to direct penetration. In conclusion, the highest viability of cells was seen on day 2 of the culture in the AgSON scaffolds, making them the best choice as a tissue engineering scaffold.

Discussion

The uniform and bead-free morphology of the nanofibers obtained is a successful confirmation of the optimization of electrospinning parameters. The β-CD incorporated PU nanofibers have been electrospun by other researchers and have obtained the same morphology and diameter distribution of nanofibers[28-29]. The contact angle analysis revealed the incorporation of β-CD in the PU nanofibers imparted hydrophilicity to the nanofibers and the lower water contact angle has been seen in other studies also where the researchers have incorporated β-CD in PU[30-31]. The reason for this can be attributed to the presence of hydrophilic components in the β-CD. The hydrophilic surface will be efficient for delivery of antimicrobial Ag NPs in tissue engineering applications. Furthermore, it will provide proper attachment surfaces for the cells to proliferate. Moreover, to check the antibacterial activity of the scaffolds with adsorbed Ag NPs two antibacterial tests were carried out, viz, disk diffusion assay and turbidity test using the bacterial strains *E. coli* and *S. aureus*. Both the Ag NPs adsorbed scaffolds (AgSON and AgHYD) showed significant antibacterial activity against both the bacteria. The antibacterial test results of this study is in total agreement with other studies of Ag NPs adsorbed nanofibers given the small size of NPs[32–34]. The biocompatibility assay on the 3T3 L1 cells also showed the increase in cell viability upon increase in the days of culture in all β-CD incorporated scaffolds. The biocompatibility of β-CD incorporated PU nanofibers due to its hydrophilicity has been seen in other studies also and is in total agreement with our results[31,35]. Given all these properties, the fabricated scaffolds are suitable for tissue engineering applications.

Conclusion

Two unique strategies for Ag NPs adsorption on the fibers were developed and a comparison between the two was made. The fiber scaffolds showed improved hydrophilicity, antibacterial activity, and cell viability. These scaffolds released Ag NPs in a controlled manner, just enough for the bacteria to die without causing damage to host cells until day 2 of the culture. These fibers are suitable for biofilm inhibition in tissue engineering applications. In the future, more potent drugs can be incorporated into our scaffolds to inhibit biofilm formation more efficiently using the aforementioned strategies.

Acknowledgement

This work was supported by the Science and Engineering Research Board (SERB) research grants (CRG/2020/000113).

Conflict of interest

The authors declare no conflict of interest.

References

1 Chao Y, Marks L R, Pettigrew M M and Hakansson A P, Streptococcus pneumoniae biofilm formation and dispersion during colonization and disease, *Front Cell Infect Microbiol*, 2014, **4**. doi:10.3389/fcimb.2014.00194.

2 Joo H S and Otto M, Molecular basis of *in vivo* biofilm formation by bacterial pathogens,*Chem Biol*, 2012, **19**(12), 1503-1513. doi:10.1016/j.chembiol.2012.10.022.

3 Bjarnsholt T, The role of bacterial biofilms in chronic infections, *APMIS J Pathol Microbiol Immunol*, 2013, **121**(s136), 1-51. doi:10.1111/apm.12099.

4 Khatoon Z, McTiernan C D, Suuronen E J, Mah T F and Alarcon E I, Bacterial biofilm formation on implantable devices and approaches to its treatment and prevention, *Heliyon*, 2018, **4**(12), e01067. doi:10.1016/j.heliyon. 2018.e01067.

5 Veerachamy S, Yarlagadda T, Manivasagam G and Yarlagadda P K, Bacterial adherence and biofilm formation on medical implants: A review, *Proc Inst Mech Eng Part H J Eng Med*, 2014, **228**(10), 1083-1099. doi:10.1177/09544119 14556137.

6 Khan R S, Rather A H, Wani T U, Rather S, Amna T, *et al.*, Recent trends using natural polymeric nanofibers as supports for enzyme immobilization and catalysis, *Biotechnol Bioeng*, 2022, **120**(1), 22-40. doi:10.1002/bit.28246.

7 Khan R S, Wani T U, Rather A H, Beigh M A and Sheikh F A, Using nanofiber scaffolds for the differentiation of induced pluripotent stem cells into cardiomyocytes: The latest approaches in tissue engineering, In: *Engineering Materials for Stem Cell Regeneration*, Springer, Singapore, 2021, 69-102. doi:10.1007/978-981-16-4420-7_4

8 Khan R S, Rather A H, Wani T U, Rather S ullah, Abdal-hay A, *et al.*, A comparative review on silk fibroin nanofibers encasing the silver nanoparticles as antimicrobial agents for wound healing applications, *Mater Today Commun*, 2022, **32**, 103914. doi:10.1016/j.mtcomm.2022.103914.

9 Sheikh F A, Kanjwal M A, Saran S, Chung W J and Kim H, Polyurethane nanofibers containing copper nanoparticles as future materials, *Appl Surf Sci*, 2011, **257**(7), 3020-3026. doi:10.1016/j.apsusc.2010.10.110.

10 Naureen B, Haseeb A S M A, Basirun W J and Muhamad F, Recent advances in tissue engineering scaffolds based on polyurethane and modified polyurethane, *Mater Sci Eng C*, 2021, **118**, 111228. doi:10.1016/j.msec.2020.111228.

11 Lukášek J, Hauzerová Š, Havlíčková K, Strnadová K, Mašek K, *et al.*, Cyclodextrin-polypyrrole coatings of scaffolds for tissue engineering, *Polymers (Basel)*, 2019, **11**(3), 459. doi:10.3390/polym11030459.

12 Cui H, Cui L, Zhang P, Huang Y, Wei Y, *et al.*, In situ electroactive and antioxidant supramolecular hydrogel based on cyclodextrin/copolymer inclusion for tissue engineering repair, *Macromol Biosci*, 2014, **14**(3), 440-450. doi:10.1002/mabi.201300366.

13 Wani T U, Khan R S, Rather A H, Beigh M A and Sheikh F A, Local dual delivery therapeutic strategies: Using biomaterials for advanced bone tissue regeneration, *J Control Release*, 2021, **339**, 143-155. doi:10.1016/j.jconrel.2021. 09.029.

14 Wani T U, Wani T A, Rather A H, Khan R S, Beigh M A,*et al.*, Incorporating poorly soluble drugs into electrospun nanofibers for improved solubility and dissolution profile. In: *Electrospun Nanofibers*, Springer, Cham, 2022, 331-349. doi:10.1007/978-3-030-99958-2_12.

15 Franci G, Falanga A, Galdiero S, Palomba L, Rai M, *et al.*, Silver nanoparticles as potential antibacterial agents, *Molecules*, 2015, **20**(5), 8856-8874. doi:10.3390/molecules 20058856.

16 Baker C, Pradhan A, Pakstis L, Pochan D J and Shah S I, Synthesis and antibacterial properties of silver nanoparticles, *J Nanosci Nanotechnol*, 2005, **5**(2), 244-249. doi:10.11 66/jnn.2005.034.

17 Tang S and Zheng J, Antibacterial activity of silver nanoparticles: Structural effects, *Adv Healthc Mater*, 2018, **7**(13), 1701503. doi:10.1002/adhm.201701503.

18 Chen C Y and Chiang C L, Preparation of cotton fibers with antibacterial silver nanoparticles, *Mater Lett*, 2008, **62**(21-22), 3607-3609. doi:10.1016/j.matlet.2008.04.008.

19 Zhang C, Yang Q, Zhan N, Sun L, Wang H, *et al.*, Silver nanoparticles grown on the surface of PAN nanofiber: Preparation, characterization and catalytic performance, *Colloids Surf A Physicochem Eng Asp*, 2010, **362**(1-3), 58-64. doi:10.1016/j.colsurfa.2010.03.038.

20 Fu J, Li D, Li G, Huang F and Wei Q, Carboxymethyl cellulose assisted immobilization of silver nanoparticles onto cellulose nanofibers for the detection of catechol, *J Electroanal Chem*, 2015, **738**, 92-99. doi:10.1016/j.jelechem. 2014.11.025.

21 Syafiuddin A, Fulazzaky M A, Salmiati S, Kueh A B H, Fulazzaky M, *et al.*, Silver nanoparticles adsorption by the synthetic and natural adsorbent materials: An exclusive review, *Nanotechnol Environ Eng*, 2020, **5**(1), 1-18. doi:10.1007/s41204-019-0065-3.

22 Pol V G, Srivastava D N, Palchik O, Palchik V, Slifkin M A, *et al.*, Sonochemical deposition of silver nanoparticles on silica spheres, *Langmuir*, 2002, **18**(8), 3352-3357. doi:10.10 21/la0155552.

23 Landau M V, Vradman L, Herskowitz M, Koltypin Y and Gedanken A, Ultrasonically controlled deposition-precipitation Co-Mo HDS catalysts deposited on wide-pore MCM material, *J Catal*, 2001, **201**(1), 22-36. doi:10.1006/jcat.2001.3227.

24 Sheikh F A, Zargar M A, Tamboli A H and Kim H, A super hydrophilic modification of poly (vinylidene fluoride) (PVDF) nanofibers: By in situ hydrothermal approach, *Appl Surf Sci*, 2016, **385**, 417-425. doi:10.1016/j.apsusc. 2016.05.111.

25 Zhang X, Sun H, Tan S, Gao J, Fu Y, *et al.*, Hydrothermal synthesis of Ag nanoparticles on the nanocellulose and their antibacterial study, *Inorg Chem Commu*, 2019, **100**, 44-50. doi:10.1016/j.inoche.2018.12.012.

26 Tang C, Sun W and Yan W, Green and facile fabrication of silver nanoparticles loaded activated carbon fibers with long-lasting antibacterial activity, *RSC Adv*, 2014, **4**(2), 523-530. doi:10.1039/c3ra44799e.

27 Tang C, Hu D, Cao Q, Yan W and Xing B, Silver nanoparticles-loaded activated carbon fibers using chitosan as binding agent: Preparation, mechanism, and their antibacterial activity, *Appl Surf Sci*, 2017, **394**, 457-465. doi:10.1016/j.apsusc.2016.10.095.

28 Kumbasar E P A, Akduman Ç and Çay A, Effects of β-cyclodextrin on selected properties of electrospun thermoplastic polyurethane nanofibres, *Carbohydr Polym*, 2014, **104**(1), 42-49. doi:10.1016/j.carbpol.2013.12.065.

29 Lee J H, Park S H and Kim S H, Fabrication of bio-based polyurethane nanofibers incorporated with a triclosan/ cyclodextrin complex for antibacterial applications, *RSC Adv*, 2020, **10**(6), 3450-3458. doi:10.1039/c9ra06992e.

30 Wu D, Feng Q, Xu T, Wei A and Fong H, Electrospun blend nanofiber membrane consisting of polyurethane, amidoxime polyarcylonitrile, and B-cyclodextrin as high-performance carrier/support for efficient and reusable immobilization of laccase, *Chem Eng J*, 2018, **331**, 517-526. doi:10.1016/j. cej.2017.08.129.

31 Sagitha P, Reshmi C R, Sundaran S P, Binoy A, Mishra N, *et al.*, β-Cyclodextrin functionalized polyurethane nano fibrous membranes for drug delivery, *J Drug Deliv Sci Technol*, 2021, **65**. doi:10.1016/j.jddst.2021.102759.

32 Rather A H, Khan R S, Wani T U, Rafiq M, Jadhav A H, *et al.*, Polyurethane and cellulose acetate micro-nanofibers containing rosemary essential oil, and decorated with silver nanoparticles for wound healing application, *Int J Biol Macromol*, 2023, **226**, 690-705. doi:10.1016/j.ijbiomac.2022.12.048.

33 Sheikh F A, Barakat N A M, Kanjwal M A, Chaudhari A A, Jung I H, *et al.*, Electrospun antimicrobial polyurethane nanofibers containing silver nanoparticles for biotechnological applications, *Macromol Res*, 2009, **17**(9), 688-696. doi:10.1007/BF03218929.

34 Jeon H J, Kim J S, Kim T G, Kim J H, Yu W R,*et al.*, Preparation of poly(ε-caprolactone)-based polyurethane nanofibers containing silver nanoparticles, *Appl Surf Sci*, 2008, **254**(18), 5886-5890. doi:10.1016/j.apsusc.2008.03.141.

35 Klempaiová M, Dragúňová J, Kabát P, Hnátová M, Koller J, *et al.*, Cytotoxicity testing of a polyurethane nanofiber membrane modified with chitosan/β-cyclodextrin/berberine suitable for wound dressing application: Evaluation of biocompatibility,*Cell Tissue Bank*, 2016, **17**(4), 665-675. doi:10.1007/s10561-016-9585-2.